Selection Rules of the Charge Transfer Mechanism of Surface-Enhanced Raman Scattering: The Effect of the Adsorption on the Relative Intensities of Pyrimidine Bonded to Silver Nanoclusters

Silvia P. Centeno, Isabel López-Tocón, Juan F. Arenas, Juan Soto, and Juan C. Otero*

Department of Physical Chemistry, Faculty of Sciences, University of Málaga, E-29071 Málaga, Spain

Received: April 5, 2006; In Final Form: June 8, 2006

Surface-enhanced Raman spectra (SERS) of pyrimidine recorded on a silver electrode have been analyzed on the basis of a resonant Raman (RR) process involving photoexcited charge transfer (CT) states of the metal−adsorbate surface complex. The main feature of the SERS of benzene and azine derivatives is the enhancement of the totally symmetric ring stretching mode 8a due to Franck−Condon contributions related to the CT transition. Although this behavior is observed in the SERS of pyrimidine, its spectrum is also characterized by the strong enhancement of the nontotally symmetric mode 8b. This peculiar feature can be explained only by the redistribution of the Franck−Condon factors between the 8ab pair of vibrations originated by the descent in symmetry occurring when pyrimidine is bonded to silver nanoclusters. This conclusion is a new evidence of the main role of the RR−CT enhancement mechanism in the SERS of aromatic molecules and shows once again the usefulness of the methodology developed by our group in order to analyze these complex spectra.

1. Introduction

Although a lot of research has been done since the discovery of surface-enhanced Raman scattering (SERS),[1] the origin of this effect has not yet been totally elucidated.[2] It is generally accepted that SERS is mainly based on the electromagnetic enhancement mechanism (EM):[3,4] the laser excitation of single or collective plasmon resonances of the metal produces massive amplifications of the electromagnetic local field a few nanometers above the surface. However, a second enhancement contribution related to the excitation of charge-transfer resonances (CT mechanism[5]) of the metal−adsorbate system must not be discarded under certain circumstances. This contribution arises from electronic coupling between the adsorbate and nanometric features on the metal. Although the CT mechanism is frequently considered a minor contribution to the global SERS enhancement, it seems to be related to the observation of single-molecule (SM) SERS reported recently by several authors,[6,7] which requires huge enhancements of the order of $10^{14}-10^{15}$. The blinking effect related to SM events has been suggested to arise from temporal interruptions of the electronic coupling between the adsorbed molecule and the metal nanostructure[8] or from fluctuations of molecule−surface charge-transfer interactions.[9] Moreover, another remarkable observation is the anti-Stokes portion of the SERS spectra, which shows line intensities much greater than expected.[10] This has been explained as due to a resonance enhancement resulting from adsorbate-silver complex charge transfer states.[11]

Despite of all these observations and the interest of SM-SERS experiences, the CT mechanism is not usually considered when analyzing a SERS spectrum. This is probably because of being a rather complex effect occurring at atomic or nanometric scale and related to transitions between the ground electronic state of the adsorbate−metal (A−M) system and charge transfer excited levels. These electronic transitions of the surface complex are very difficult to be observed directly,[12] and they have been reported in very few cases.[13] As a result, these excited CT states are not characterized at all, the only information available being their energies, which usually lie in the range of the visible photons used in Raman spectroscopy. In addition, the interpretation of SERS from the point of view of the CT mechanism is a complicated task as there exist no general selection rules; on the contrary, the SERS−CT enhanced vibrations depend on the particular properties of the electronic states involved in the CT process of a particular A−M system.

On this concern, our group has developed a systematic methodology[14] to detect and estimate quantitatively the CT contribution to a particular SERS spectrum. It is mainly based on the comparison between the experimental relative intensities and theoretical estimations derived from ab initio calculations. Generally speaking, we assume a CT mechanism of SERS similar to a resonance Raman process (RR−CT) having only two steps. In step 1, the laser photon ($h\nu$) produces the resonant transfer of one electron from the metal (M) to vacant orbitals of the adsorbate (A) yielding the excited CT state ($A^-−M^+$):

$$\text{Step 1: } A-M + h\nu \rightarrow A^- - M^+$$

When the electron comes back to the metal in step 2, a Raman photon ($h\nu'$) can be emitted if the molecule remains vibrationally excited (A*):

$$\text{Step 2: } A^- - M^+ \rightarrow A^* - M + h\nu'$$

The enhanced vibrations in RR are related to differences between the equilibrium geometry and gradients (vibrational wavenumbers) of the potential energy surfaces (PES) of the involved electronic states, and accounting for the Franck−Condon (A-term) and the Herzberg−Teller (B-term) contributions[15] relevant in all electronic spectroscopies. As can be seen,

* Corresponding author: E-mail: jc_otero@uma.es. Fax: +34952132047.

10.1021/jp0621373 CCC: $33.50
Published on Web 07/07/2006

this metal-to-ligand CT process involves the transient formation of the radical anion (A^-) of neutral adsorbates such as benzene or pyrimidine if a complete electron is transferred into the excited state. Given that CT states of aromatic molecules are very little known, we have resorted to ab initio calculations to get insight into their properties. On this basis, we have been able to explain the SERS of pyrazine, pyridine, and benzene derivatives recorded on silver colloids and on a roughened Ag electrode as well as their dependence on the electrode potential.[14] The main feature of CT processes in the SERS spectra of these aromatic benzene-like molecules is the very strong enhancement of the totally symmetric ring stretching mode 8a;ν_{ring};A_1 recorded in the 1600 cm^{-1} region and being the strongest band in many cases.[14,16] Although this fundamental is also enhanced in the SERS of pyrimidine, it does not reach as much intensity as in the SERS of related molecules, e.g., pyrazine; on the contrary, its relative intensity is similar to that of ring stretching mode 8b;ν_{ring};B_2 at many of the applied electrode potentials. The strong intensity of this nontotally symmetric fundamental is the main feature of the SERS of pyrimidine. It will be demonstrated that the strong enhancement of mode 8b is due to the asymmetric adsorption of pyrimidine. The formation of the surface complex produces the descent of the relevant symmetry from C_{2v} to C_s and the mixing between both normal modes.

2. Theoretical Basis

The main conclusions we have established in previous works[14] can be summarized as follows. (1) The CT mechanism is the main responsible for the SERS relative intensities observed in some SERS of benzene-like molecules such as pyrazine, pyridine, and derivatives. (2) In the excited CT state, the adsorbed species must be similar to the respective radical anion, given that the ab initio computed properties of this molecular species account satisfactorily for the observed behavior. (3) The participation of a second excited CT state is also detected in the SERS of pyrazine and pyridine. This is not surprising since the ground electronic state of the benzene radical anion is doubly degenerate. (4) The CT electronic transitions seem to obey symmetry-based selection rules similar to those of the electric dipole radiation mechanism; this points to an exclusively photonic process[2] like the above-described RR−CT mechanism and would discard the involvement of nonradiative steps such as electron transfer.[14c] (5) The ab initio energies of the CT transitions of the surface complex are in good agreement with the energies of the visible laser photons used in Raman.[14d] (6) Finally, a local symmetry restricted to the vicinity of the adsorption site has been observed to be the relevant one. In this respect the appearing in SERS of Raman silent modes can be explained taking into account the surface complex formation without resorting to effects related to electric field gradient in the interphase.[14c] This effect of the adsorption on the CT process is envisaged to be more important in those systems with a lower symmetry and with CT states closer in energy, as it is the case of pyrimidine. For instance, the formation of the surface complex does not affect the symmetry of the adsorbate in pyridine (C_{2v}). In turn, in pyrazine it does, yielding a descent from D_{2h} to C_{2v}, while in pyrimidine (C_{2v}) it affects much more strongly, yielding a descent until C_s (Figure 1).

2a. The Theoretical Model. Two approaches have been followed in order to analyze CT processes in the SERS of pyrimidine. In the first case only the adsorbate is taken into account in the calculations. We have studied two possible CT transitions between the neutral molecule in its electronic ground-state S_0:$^1A_1$ and the radical anion in its ground and first excited levels, called D_i states given that they are doublets (D_0;$^2A_2$ and D_1;$^2B_1$ respectively[17]). In the RR-CT mechanism, such states of the molecule should be considered as states of the pyrimidine-silver complex, but labeled from the point of view of the adsorbate. In previous works[14] on the SERS-CT of pyrazine, pyridine, and derivatives, we found that the ab initio calculations of the relevant electronic properties of the neutral molecules and their radical anions do not depend significantly on the level of theory. On this basis, we have carried out RHF and UHF calculations for the neutral molecule and the radical anion, respectively, using the 3-21G and LanL2DZ basis sets in order to compare them with the ones obtained for the pyrimidine−silver supermolecule. The LanL2DZ basis set (D95[18] for the first row atoms and the Los Alamos plus DZ effective core pseudopotential[19] for the remaining ones) has been selected in order to take into account possible relativistic effects in the silver atoms.

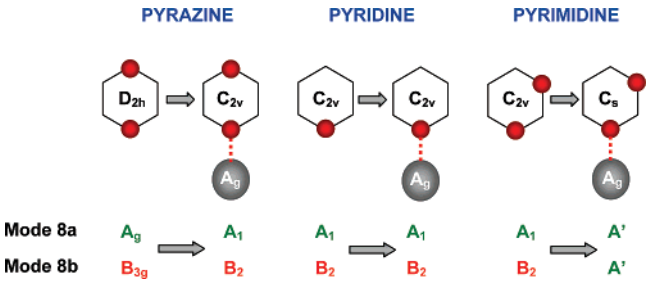

Figure 1. Effect of the adsorption on the molecular symmetry of pyrazine, pyridine, and pyrimidine and the respective vibrations 8a and 8b.

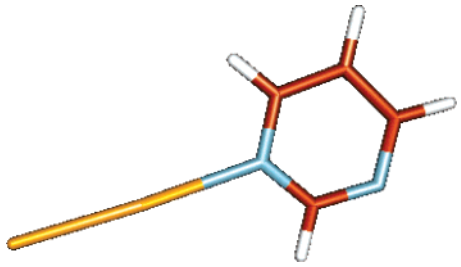

Figure 2. RHF/LanL2DZ optimized geometry of the pyrimidine−Ag_2 complex in the S_0;$^1A'$ ground electronic state.

In the second approach, the properties of the ground and excited states of the metal−adsorbate system have been studied. The nature of SERS-CT adsorption sites is not yet well known, though it seems to be related to some atomic clusters or nanostructures located on the metal surface.[20] The pyrimidine−Ag_2 system has been used to model the surface complex (Figure 2). This is the same than in the previous study on pyrazine[14d] where its usefulness was already demonstrated. The neutral Ag_2 cluster is a closed-shell system suitable for CIS calculations that are known to yield results with a reliability equivalent to that of HF results in the ground state.[21] Moreover, the Ag_2 system is compatible with the electrode potential at which the CT processes are observed, ca. −0.5 V, which coincides with the zero charge potential of the silver electrode. CIS/3-21G and LanL2DZ calculations of the first 10 singlets, including two CT states, of the pyrimidine−Ag_2 complex have been carried out.

The bonding of the Ag_2 cluster with the lone electron pair of one of the nitrogen atoms means a perpendicular orientation of the pyrimidine ring with respect to the metal surface. This bonding originates a shift of the calculated vibrational wavenumbers of the complexed pyrimidine with respect to the

isolated molecule similar to that observed between the Raman and SERS records as in the case of pyrazine.[14e] Despite of all this, the selected pyrimidine−Ag_2 model might be considered too simple in order to model an irregular and rough macroscopic surface. However, its ability to explain the SERS results validates it completely. All the ab initio calculations have been carried out using the GAUSSIAN 98 package.[22]

2b. Method of Analysis. In our previous studies we found that the A-term (Franck−Condon contribution) determines the relative enhancement of the RR-CT bands, while the B-term (Herzberg−Teller contribution) is of much less importance.[14c] The relative intensity of a band in RR can be estimated by means of the Peticolas' equation,[23] given that the A-term depends mainly on the differences between the equilibrium geometries ($\Delta Q \neq 0$) of the molecule in the electronic states involved in the resonant transition:

$$I_n = k(\Delta Q_{i0,n})^2 (\nu_{0,n})^3 \quad (1)$$

The intensity I_n of the nth normal mode depends on $\Delta Q_{i0,n}$, the displacement between the equilibrium geometries of both the excited "i" and the ground "0", electronic states expressed along each normal mode, and on its wavenumber in the ground state $\nu_{0,n}$. The term k is constant for all the modes and can be adjusted to normalize relative values. The normal mode displacements $\Delta Q_{i0,n}$ are calculated as follows:

$$\Delta Q_{i0,n} = L_0^{-1} \Delta R_{i0} \quad (2)$$

L_0^{-1} is the inverse of the ground-state normal modes L-matrix obtained from ab initio force field calculations, and the vector ΔR_{i0} contains the differences between the optimized structures of both states expressed in the same set of internal coordinates used to calculate the L-matrix.

3. Experimental Section

The experimental conditions under which the SERS spectra were recorded have been detailed elsewhere.[14] Briefly, after polishing the silver surface of the working electrode, this was electrochemically activated by maintaining the electrode potential at −0.5 V and then subjecting it to ten, 2 s pulses at +0.6 V. During this procedure a 1 M aqueous solution of KCl has been employed as electrolyte. A PAR model 173/175 potentiostat/programmer was used to control the three-electrode cell fitted with a platinum counter electrode, a saturated Ag/AgCl/KCl reference electrode, and the pure silver working electrode. Raman and SERS spectra have been recorded in a Jobin-Yvon U-1000 spectrometer fitted with a cooled Hamamatsu 943-03 photomultiplier using the 514.5 nm exciting line from a Spectra Physics 2020 Ar^+ laser with an effective power of 30 mW reaching the sample.

Figure 3 shows the Raman spectrum of the 1 M aqueous solution of pyrimidine as well as the SERS records on silver at electrode potentials ranging from 0 to −1.00 V obtained from an aqueous solution 0.1 M in KCl and $5 \cdot 10^{-3}$ M in pyrimidine. Raman and SERS intensities and wavenumbers are available in Table 1. Vibrational assignment of Raman spectrum was made on the basis of the scaled B3LYP/6-31+G* force field of pyrimidine following the Pulay's SQMFF methodology[24] in the independent set of internal coordinates collected in Table 1S and Figure 1S from the Supporting Information. Additionally, previous reports on the assignment of the vibrational spectrum of pyrimidine have been considered.[25]

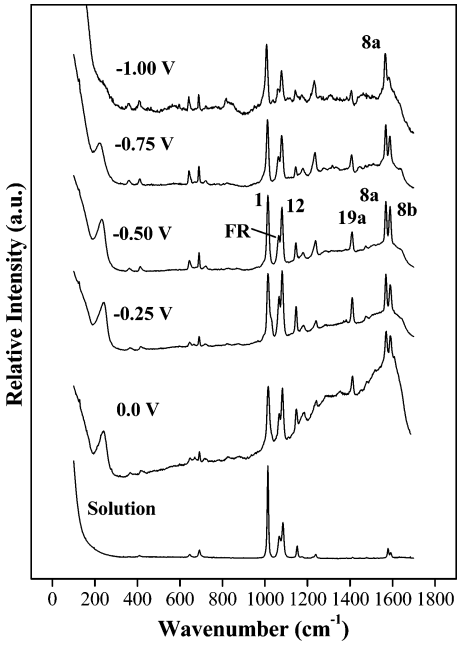

Figure 3. Raman spectrum of the aqueous solution and SERS spectra of pyrimidine recorded on silver at different electrode potentials.

It can be seen that the main features of the Raman spectrum are the very strong band at about 1000 cm^{-1} corresponding to mode 1;ν_{ring};A_1 and the two medium intensity bands assigned to mode 12;ν_{ring};A_1 and a combination band in Fermi resonance (FR), respectively. However, the SERS relative intensities are very different since modes 19a;δ(CH);A_1, 8a;ν_{ring};A_1, and 8b;ν_{ring};B_2 are clearly enhanced in the 1600−1400 cm^{-1} region. These enhancements are more evident when the electrode potential is made more negative, being the most important feature in the SERS spectra. Mode 1 remains to be the strongest band in any SERS record and its relative intensity with respect to mode 12 does not change noticeably but at negative electrode potentials.

4. Discussion

4a. RR-CT Intensities of Isolated Pyrimidine. Table 2 summarizes the HF/LanL2DZ ΔQ displacements and relative intensities calculated for the $D_0-S_0;{}^2A_2-{}^1A_1$, and $D_1-S_0;{}^2B_1-{}^1A_1$ transitions of the isolated molecule. HF/3-21G results have been avoided in the discussion for simplicity but are available in the Supporting Information (Table 2S). Given that the radical anion belongs to the same symmetry point group as the neutral molecule (C_{2v}), only the totally symmetric modes have nonzero ΔQ displacements. Significant ΔQ values corresponding to the $D_0-S_0;{}^2A_2-{}^1A_1$ transition are calculated for the 8a, 19a, and 1 modes amounting to −0171, −0.120, and −0.239 $amu^{1/2}$ Å, respectively, and yielding the relative RR-CT intensities of 100, 34, and 45, respectively. The experimental SERS intensities of the record at −0.75 V amount to 100, 45, and 155, respectively, and therefore, it is clear that theoretical results account for the enhancement of these vibrations but the experimental intensity of mode 1 is larger than the calculated intensity. A similar result is obtained for mode 12, which shows medium intensity though no significant CT enhancement is expected. Mode 12 and, particularly, mode 1 show always high intensities in SERS spectra, similar to those observed in the Raman records. This behavior has also been observed by other authors such as Sinclair[16a] and Muniz-Miranda et al.[16d] Additionally, modes 1 and 12 SERS intensities do not depend noticeably on the

TABLE 1: Experimental and B3LYP/6-31+G* Scaled Vibrational Wavenumbers, Relative Intensities of the Aqueous Solution Raman Spectrum and of the SERS Spectra, and Assignment of the Vibrational Spectrum of Pyrimidine

Raman			SERS (V)													
liquid	solution		0.00		−0.25		−0.50		−0.75		−1.00		B3-LYP/6-31+G* scaled[a]			
ν[b]	ν	I	ν	I	ν	I	ν	I	ν	I	ν	I	ν	% PED[c]	mode[d]	C_{2v}
3092	3108	71											3051	100ν(C′H)	7b,ν(CH)	B_2
3080	3086	160											3085	10ν(C′H),89ν(C*H)	20a,ν(CH)	A_1
3056	3076	286	3060	64	3054	64	3056	57	3056	59	3054	25	3069	98ν(CH)	2,ν(CH)	A_1
3044	3062	151	-										3047	90ν(C′H),10ν(C*H)	13,ν(CH)	A_1
1576	1588	57	1586	86	1584	74	1584	84	1582	75	1578	32?	1569	28ν(CN),40ν(C′C*),9δ(CH),8δ(C*H)	8b,ν_{ring}	B_2
1568	1574	100	1566	100	1564	100	1564	100	1564	100	1562	100	1572	42ν(C′N),18ν(C′C*),26δ(C′H)	8a,ν_{ring}	A_1
1470	1474	12?[e]											1463	18ν(C′N),34δ(CH),14δ(C′H),22δ(C*H)	19b,δ(CH)	B_2
1402	1408	14?	1408	74	1406	69	1406	49	1404	45	1402	35	1406	30ν(CN),14ν(C′N),48δ(C′H)	19a,δ(CH)	A_1
													1368	44δ(CH),48δ(C′H),7δ(C*H)	δ(CH)	B_2
1231	1233	43	1237	35	1235	22	1233	43	1231	50	1229	42	1217	44ν(CN),32δ(C′H),18δ(C*H)	ν_{ring}	B_2
1160	1168	20?	1178	35	1176	19?	1174	14?	1172	17?	1170	17?	1150	28ν(CN),46ν(C′N),22ν(C′C*)	ν_{ring}	B_2
1140	1146	129	1142	87	1140	71	1140	43	1138	25	1138	25?	1136	32ν(CN),14ν(C′C*),18δ(C′H)31δ_r	ν_{ring}	A_1
													1066	12ν(CN),16ν(C′N),24ν(C′C*),44δ(CH)	δ(CH)	B_2
1077	1077	374	1077	203	1073	174	1073	134	1073	113	1071	73	1056	44ν(C′C*),10δ(C′H),43δ_r	12,δ_{ring}	A_1
1055	1059	231	1059	116	1059	109	1057	63	1057	60	1055	36			(10b+16b)FR	A_1
													1004	32γ(CH),40γ(C′H),13γ(C*H)16τ_r	5,γ(CH)	B_1
993	1007	974	1009	235	1007	178	1007	157	1005	155	1001	150	990	24ν(CN),24ν(C′N),14ν(C′C*)38δ_r	1,ν_{ring}	A_1
													983	92γ(C′H)	17a,γ(CH)	A_2
													963	48γ(CH),18γ(C′H),24γ(C*H)10τ_r	11,γ(CH)	B_1
													806	11γ(CH),46γ(C′H),22γ(C*H)20τ_r	10b,γ(CH)	B_1
													719	26γ(C*H),71τ_r	4,τ_{ring}	B_1
680	684	71	684	40?	682	26	682	37	682	46	682	32	684	91δ_r	6a,δ_{ring}	A_1
624	638	31	640	25?9	638	12	636	20	636	32	634	26	624	88δ_r	6b,δ_{ring}	B_2
400	402	20?	408	14?	408	8?	406	8?	404	16?	402	24?	400	92τ_r	16a,τ_{ring}	A_2
			357	13?	357	6?	353	6?	353	12?	351	21?	345	12γ(C*H),83τ_r	16b,τ_{ring}	B_1

[a] Scaled force field. [b] Wavenumbers in cm^{-1}. [c] PED: Potential energy distribution matrix. See Supporting Information for atom labeling and internal coordinate definitions. [d] Wilson's nomenclature; ν stretching, δ in-plane deformation, γ out-of-plane deformation, τ torsion. [e] Intensities labeled with a "?" correspond to weak or broad bands.

TABLE 2: Calculated (LanL2DZ) ΔQ Displacements and Relative Intensities Related to $D_{i=0,1}-S_0$ Transitions of Isolated Pyrimidine (Prm) and $CT_{i=0,1}-S_0$ Transitions of the Surface Complex (Prm−Ag_2)

			Prm								Prm-Ag_2			
			D_0-S_0 $^2A_2-{}^1A_1$		D_1-S_0 $^2B_1-{}^1A_1$		D_0-S_0 $^2A_2-{}^1A_1$		D_1-S_0 $^2B_1-{}^1A_1$		CT_0-S_0 $2^1A''-1^1A'$		CT_1-S_0 $3^1A''-1^1A'$	
C_{2v}	C_s	mode[a]	ΔQ[b]	I[c]	ΔQ[b]	I[c]	ΔQ[d]	I[c]	ΔQ[d]	I[c]	ΔQ[e]	I[c]	ΔQ[e]	I[c]
A_1	A′	20a,ν(CH)	0.003	0	0.004	1	−0.002	0	−0.005	1	0.002	0	0.002	0
		2,ν(CH)	0.011	3	−0.002	0	0.011	5	−0.002	0	0.001	0	0.002	1
		13,ν(CH)	0.004	1	−0.009	2	−0.005	1	0.010	3	−0.006	2	−0.005	4
		8a,ν_{ring}	**−0.171**	**100**	**0.177**	**100**	**−0.137**	**100**	**0.142**	**100**	**−0.052**	**18**	**−0.069**	**100**
		19a,δ(CH)	−0.120	34	0.127	36	0.121	55	−0.132	60	0.068	23	0.068	70
		ν_{ring}	−0.046	3	−0.058	4	0.042	3	0.050	5	0.065	11	0.039	12
		12,δ_{ring}	−0.065	4	−0.067	4	0.054	5	0.055	4	0.035	3	0.029	5
		1,ν_{ring}	−0.239	45	−0.225	37	0.245	74	0.229	60	0.150	36	0.110	61
		6a,δ_{ring}	0.096	3	0.065	1	0.090	3	0.059	1	0.085	4	0.046	4
B_2	A′	7b,ν(CH)					0.001	0	−0.001	0	0.002	0	−0.000	0
		8b,ν_{ring}					**0.096**	**49**	**−0.102**	**52**	**0.120**	**100**	**0.061**	**82**
		19b,δ(CH)					0.000	0	−0.002	0	−0.014	1	−0.011	2
		δ(CH)					−0.003	0	0.005	0	−0.010	1	−0.002	0
		ν_{ring}					0.008	0	0.001	0	−0.072	16	−0.033	10
		ν_{ring}					−0.004	0	−0.015	0	−0.027	2	−0.020	3
		δ(CH)					−0.010	0	−0.012	0	−0.067	10	−0.053	18
		6b,δ_{ring}					−0.018	0	−0.013	0	0.071	2	0.012	0

[a] Wilson's nomenclature; ν stretching, δ in-plane deformation, γ out-of-plane deformation, τ torsion. [b] From eq 2 in $amu^{1/2}$ Å. [c] From eq 1. [d] ΔQ displacements calculated with the ΔR vector of the isolated molecule and the L^{-1} matrix of the surface complex. [e] ΔQ displacements calculated with the ΔR vector and the L^{-1} matrix of the surface complex.

electrode potential, especially mode 1. All of this seems to point to an important electromagnetic contribution to the SERS intensity of these two vibrational modes.[14c,g]

Very similar RR-CT intensities are obtained for the D_1-S_0;$^2B_1-{}^1A_1$ transition, and therefore it is not possible to deduce which transition is responsible for the observed SERS intensities. Despite this, it can be deduced that an electronic process involving the excitation of the surface complex to charge-transfer states similar to the doublet states of the radical anion of pyrimidine is responsible for the strong SERS enhancement of modes 8a and 19a. However, the enhancement of the in-plane mode 8b;ν_{ring};B_2, which shows relative intensities similar to those of mode 8a;ν_{ring};A_1 in some spectra, is not explained under this RR-CT mechanism operating in the isolated adsorbate.

4b. Effects of the Adsorption on the Electronic Properties of Pyrimidine. The activity of this vibration may be related to the descent in symmetry when the pyrimidine is bonded to the silver surface, given that modes B_2 become totally symmetric

TABLE 3: Wavenumber Shifts ($\Delta\nu$) between the SERS of Pyrimidine (Prm) Recorded at −0.50 V and the Raman of the Pure Liquid and RHF/LanL2DZ Calculated Shifts between the Vibrations of the Surface Complex (Prm−Ag_2) and the Isolated Molecule (Prm)

		experimental			RHF/LanL2DZ		
		Raman liquid	SERS −0.50 V		Prm C_{2v}	Prm−Ag_2 C_s	
C_{2v}	mode[a]	ν[b]	ν	$\Delta\nu$	ν	ν	$\Delta\nu$
A_1	8a,ν_{ring}	1568	1564	−4	1751	1745	−6
	19a,δ(CH)	1402	1406	4	1552	1556	4
	ν_{ring}	1140	1140	0	1244	1248	4
	12,δ_{ring}	1077	1073	−4	1156	1161	5
	1,ν_{ring}	993	1007	14	1073	1081	8
	6a,δ_{ring}	680	682	2	748	751	3
B_2	8b,ν_{ring}	1576	1584	8	1749	1762	13
	19b,δ(CH)	1470			1615	1618	3
	δ(CH)				1510	1514	4
	ν_{ring}	1231	1233	2	1345	1350	5
	ν_{ring}	1160	1174?[c]	?	1212	1211	−1
	δ(CH)				1175	1180	5
	6b,δ_{ring}	624	636	12	690	698	8

[a] Wilson's nomenclature; ν stretching, δ in-plane deformation, γ out-of-plane deformation, τ torsion. [b] Wavenumbers in cm^{-1}. [c] Wavenumbers labeled with a "?" correspond to weak or broad bands.

(A′) under C_s. The formation of the pyrimidine−silver complex can be deduced from Table 3 where the observed shifts ($\Delta\nu$) between the wavenumbers of the Raman spectrum of the pure liquid and the SERS record at −0.5 V are compared to those calculated between the isolated molecule (C_{2v}) and the pyrimidine−Ag_2 system (C_s) (RHF/LanL2DZ). Except the 8a and 12 modes, it can be seen that the in-plane vibrations shift to higher frequencies in the SERS, and that the largest blue shifts correspond to the fundamentals 1, 8b, and 6b. This experimental behavior is compatible with the RHF/LanL2DZ calculated shifts for the adsorption through the lone electron pair of one of the heteroatoms, like pyrazine[14e] and pyridine[26] do. RHF/3-21G results are similar. The shifts of mode 12 and the band at 1160 cm^{-1} are not meaningful, since the former is involved in a Fermi resonance with a combination band, while the latter is very weak, broad, and asymmetric due to the overlapping of two bands.

All this points to a perpendicular orientation of pyrimidine ring with respect to the metal surface yielding a planar C_s structure. The adsorption can lead to three possible effects: (1) the normal mode rotation of the vibrations, affecting L^{-1} matrix; (2) the descent in the symmetry of the structure of pyrimidine, affecting ΔR, and (3) the mixing between both CT states and/or with other states of the metal. Therefore, the SERS activity of vibration 8b can be due to the mentioned effects 1 and/or 2 originated by the absorption, and they will be discussed in sections 4c and 4e, respectively.

4c. Effects of the Adsorption on the Force Field. The descent in symmetry of the molecule can cause the normal mode rotation (effect 2, section 4b) and, therefore, the redistribution of the CT contributions between vibrations of similar frequencies but with different symmetry under C_{2v}, becoming of the same symmetry under C_s. To estimate this effect, the ΔQ have been recalculated by combining the previous ΔR values calculated for the two D_i-S_0 transitions of the isolated pyrimidine with the corresponding L^{-1} matrix of the pyrimidine−Ag_2 complex (Tables 2 and 2S). It can be seen that the so calculated ΔQ are very similar to those of the isolated molecule for all A_1 fundamentals (A′ in the complex) with the exception of the mode 8a. For the D_0-S_0 transition, its ΔQ is reduced from ca. −0.171 $amu^{1/2}$ Å in the isolated case to −0.137 $amu^{1/2}$ Å when using the L^{-1} of the surface complex. Although the B_2 fundamentals have now non zero ΔQ displacements (A′ in the complex), only mode 8b shows a significant value amounting to ca. 0.096 $amu^{1/2}$ Å. These results show that the adsorption of pyrimidine originates the mixing between the vibrations 8a and 8b. This mode rotation leads to the redistribution of the Franck−Condon contribution between both fundamentals. This explains why this pair of vibrations has similar SERS intensities and why mode 8a is weaker than expected from the CT intensities calculated for the isolated molecule.

Moreover, this model also accounts for the differentiated behavior observed in the SERS of similar molecules. In pyrazine[14a,d] (D_{2h}) and pyridine[14b] (C_{2v}), mode 8b remains non-totally symmetric (B_2 under C_{2v}) when the surface complex is formed, and therefore the mixing with mode 8a is not possible (Figure 1). This is why mode 8a shows the strongest enhancement in the SERS of pyrazine or pyridine while mode 8b is so weak, just the opposite to what happens in pyrimidine.

4d. Singlet States of the Pyrimidine−Ag_2 System and CT Transitions. To confirm these results, we have carried out CIS/LanL2DZ and 3-21G calculations of the pyrimidine−Ag_2 cluster, taking the equilibrium structure of the electronic ground state $S_0;{}^1A'$ as the starting point. Tables 4 and 3S show the respective LanL2DZ and 3-21G energies, oscillator strengths, and relevant charges corresponding to the Franck−Condon points (FCP) of the first 10 singlets as well as to the optimized structures of the A″ excited states. The CIS/LanL2DZ excited singlets are in the order $2^1A'$, $3^1A'$, $1^1A''$, $2^1A''$, $4^1A'$, $3^1A''$, $4^1A''$, $5^1A'$, $6^1A'$. Two $^1A''$ levels of the pyrimidine−Ag_2 complex (C_s) are CT states where the adsorbate has a structure very similar to that of the radical anion in the $^2A_2$ and $^2B_1$ doublet states (C_{2v}). By inspection of the Mulliken population analysis, the $S_4;2^1A''$ and $S_7;4^1A''$ singlets can be considered to be charge transfer states indeed. Such states lie about 4.05 and 4.56 eV over the ground $S_0;1^1A'$ state, respectively, and the Ag_2 cluster shows charges of 0.77 and 0.82, respectively. This implies a charge transfer from the metal to pyrimidine (Δq) amounting to −0.82 and −0.87, respectively, given that the Ag_2 cluster has a charge of −0.05 in S_0. These values of transferred charge support the proposed RR-CT mechanism where one complete electron is supposed to be transferred in step 2. Moreover, the calculated energy gap between the two CT states (0.51 eV) is very similar to that of doublet states in the radical anion (0.46 eV). The CIS/3-21G results (Table 3S) are similar: the two CT states, namely, $S_4;2^1A''$ and $S_8;4^1A''$, lie 3.99 and 4.56 eV over S_0 and have Δq values of −0.63 and −0.87, respectively. It can also be seen that the remaining singlets arise from excitations inside the Ag_2 portion of the supermolecule and show small Δq values, as low as −0.13, and therefore cannot be considered as CT states.

As can be seen in Table 4, the $S_6;3^1A''$ and $S_7(CT_1);4^1A''$ singlets lie very close (4.27 and 4.56 eV, respectively). The small energy gap is responsible for the mixing between both levels when the optimization of the respective geometries is carried out (effect 3, section 4b). This behavior has been previously observed in the CIS singlets of the pyrazine−Ag_2[14d] system and it is expected to occur when states of the same symmetry have close energies. This is responsible for the significant increase in the oscillator strength (f) of the respective CIS/LanL2DZ CT optimized states and for the noticeable decrease in the transferred charge (Δq), from −0.87 (FCP) to −0.47 (optimized), corresponding to the CT_1 state. This is also responsible for the two CIS/3-21G singlets $S_6;3^1A''$ and

TABLE 4: CIS/LanL2DZ Calculated Excitation Energies (ΔE), Oscillator Strengths (f), and Charges Related to the First Ten Singlets of the Pyrimidine−Ag_2 Complex

Data corresponding to the respective Franck−Condon points

	S_0 $1\,^1A'$	S_1 $2\,^1A'$	S_2 $3\,^1A'$	S_3 $1\,^1A''$	$S_4(CT_0)$ $2\,^1A''$	S_5 $4\,^1A'$	S_6 $3\,^1A''$	$S_7(CT_1)$ $4\,^1A''$	S_8 $5\,^1A'$	S_9 $6\,^1A'$
$\Delta E(S_i-S_0)$/eV	0.0	3.01	3.27	3.32	4.05	4.25	4.27	4.56	4.63	5.17
f^a	0.0	0.734	0.432	0.454	0.007	0.023	0.016	0.000	0.027	0.215
Ag_2 charge (q)^b	−0.05	−0.07	−0.08	−0.06	0.77	−0.09	−0.07	0.82	−0.18	−0.09
Δq^c		0.02	0.03	0.01	−0.82	0.04	0.02	−0.87	0.13	0.04

Data corresponding to the optimized geometries of the A″ singlets

	S_0 $1\,^1A'$	S_3 $1\,^1A''$	$S_4(CT_0)$ $2\,^1A''$	$S_7(CT_1)$ $3\,^1A''$	S_6 $4\,^1A''$
$\Delta E(S_i-S_0)$/eV	0.0	3.25	3.33	3.52	4.13
f^a	0.0	0.449	0.086	0.183	0.029
Ag_2 charge (q)^b	−0.05	−0.06	0.82	0.42	−0.08
Δq^c		0.01	−0.87	−0.47	0.03

[a] Oscillator strength for S_i-S_0 transitions. [b] Mulliken population corresponding to the Ag_2 cluster. [c] Transferred charge from Ag_2 to pyrimidine in S_i.

$S_8(CT_1)$;$4^1A''$ yielding the same optimized state with non-CT characteristics (Table 3S). The equilibrium structure corresponding to the CT_0 state is computed at 3.32 eV, very similar to the energy calculated with the LanL2DZ basis set. Such state is only 0.19 eV more stable than the CT_1 level that lies at 3.52 eV over S_0. Taking into account that CIS calculations systematically overestimate the electronic transition energies[21] and that CIS/LANL2DZ energies are about 25% higher than the experimental values,[27] it can be deduced that the incident photons (514.5 nm, ca. 2.5 eV) seem to be capable of exciting the pyrimidine−silver system up to the CT states. In addition, both CT_i-S_0 ($^1A''-^1A'$) transitions are allowed by the selection rules of the electric dipole radiation mechanism showing nonzero oscillator strengths and, therefore, these CT states seem to be accessible under the actual experimental conditions.

4e. RR-CT Intensities of the Pyrimidine−Ag_2 Complex. Table 2 shows the CIS/LanL2DZ normal mode displacements ΔQ and relative RR-CT intensities calculated for the CT_0-S_0;$2^1A''$-$1^1A'$ and CT_1-S_0;$3^1A''$-$1^1A'$ CT transitions of the pyrimidine−Ag_2 complex (effects 1 and 2, section 4b). CIS/3-21G results corresponding to the CT_0-S_0;$2^1A''$-$1^1A'$ transition are available in Table 2S. Generally speaking, it can be seen that ΔQ of A_1 vibrations remain bigger than those of the B_2 vibrations but smaller than those estimated for the isolated molecule, while the opposite occurs for the B_2 fundamentals. The relative RR-CT intensities calculated for the CT_1-S_0 transition are similar to those estimated considering exclusively the effect of adsorption on L^{-1}. The vibrations 8ab have relative intensities of 100 and 82, respectively, and should be the strongest enhanced vibrations; modes 19a and 1 also show significant intensity of 70 and 61, respectively. On the contrary, the calculated intensities for the resonance process with CT_0 state look very different from this picture, since mode 8b is almost the only vibration predicted to be relatively enhanced given that mode 1 shows an intensity of 36.

4f. Effect of the Electrode Potential on the Relative Intensities of Modes 8ab. All this confirms that the strong SERS intensity of mode 8b is due to the redistribution of Franck−Condon contributions between the vibrations 8ab occurring when the pyrimidine is adsorbed on the surface. However, in the SERS recorded at −0.75 V and, especially, at −1.00 V, a clear enhancement of the relative SERS intensity of mode 8a with respect to that of 8b and 19a modes can be seen. These relative intensities are in agreement with the calculated ones when considering the isolated molecule (Tables 2 and 2S) where mode 8a is expected to show the strongest enhancement. This can be explained if we consider the effect of the electrode potential on the strength of the adsorption. The A−M surface bonding is formed by donation of charge from the lone electron pair of one of the nitrogen atoms to the metal, as could be shown in the previous work on pyrazine.[14e] The extent of the donation depends in turn on the surface excess charge and, therefore, on the electrode potential. The surface complex is weaker as the potential is made more negative, given that the SERS wavenumbers tend to become similar to those of the pure Raman at negative potentials as it occurs in pyrazine.[14e] This can be seen in Figure 4, where the dependence of the shifts between the wavenumbers of the pure liquid Raman and SERS spectra on the electrode potential is shown. It means that mixing between both 8ab modes is reduced and the properties of the pyrimidine return to be those of the isolated species rather than the complexed one. This electrostatic effect is expected to be more important in pyrimidine than in pyrazine, given that it has a nonzero dipole moment. In relation to this, it has to be mentioned that the geometry of the pyrazine−Ag^{-1} cluster dissociates at the RHF/LanL2DZ level, whereas the ground state of the pyrazine−Ag_3^{-1} is a bonded state. On the contrary, the pyrimidine−Ag_3^{-1} dissociates already in the optimization process.

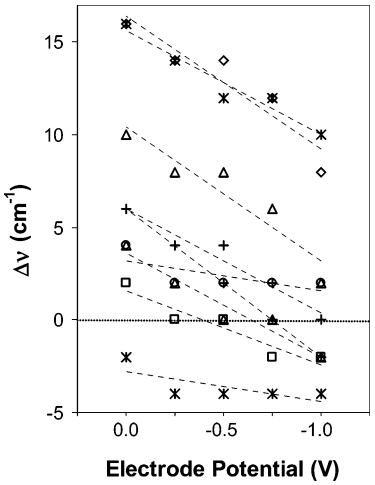

Figure 4. Dependence of the shifts ($\Delta\nu$) between the wavenumbers of the pure liquid Raman and SERS spectra on the electrode potential. Only results of bands with significant intensities are shown.

5. Conclusions

The SERS spectra of pyrimidine are compatible with a resonance Raman mechanism involving the ground electronic state of the surface complex and excited levels arising from charge transfer between the metal and the adsorbate. We have shown that such CT states have energies of the same order of the incident photon, and therefore it is possible to reach them from the ground electronic state of the surface complex. Moreover, the CT levels are similar to the doublet states in the radical anion of the isolated molecule, namely, the D_0 and D_1 states, as we have already found for other related molecules. However, the low symmetry of pyrimidine−silver complex and the small gap existing between CT states lead to a significant vibrational mode rotation and CT states mixing that perturb the electronic properties of the involved levels. A clear evidence of this effect is the strong SERS intensities recorded for the nontotally symmetric mode 8b, similar to those of mode 8a, which is usually the strongest enhanced vibration and the most characteristic feature in the SERS of benzene-like molecules. Finally, this work confirms the relevance of CT mechanism in the SERS of aromatic molecules, being possible to apply this technique to study the corresponding CT states. It also sheds some light on the origin of the SERS phenomenon and demonstrates the usefulness of the methodology we have proposed in order to understand these complex spectra.

Acknowledgment. The authors wish to express their gratitude to MEC for financial support through the projects BQU2003-1353 and NAN2004-09312-C03-01. S.P.C. gratefully acknowledges financial support through an Spanish grant from MEC.

Supporting Information Available: Figure and Table showing the selected internal coordinates and the corresponding scale factors used to refine the B3-LYP/6-31+G* force field of pyrimidine molecule. Table showing calculated (HF and CIS/3-21G) normal mode displacements and relative SERS intensities related to the CT transitions of the isolated molecule and in the surface complex. Table showing CIS/3-21G calculated excitation energies, oscillator strengths, and charges related to the first 10 singlets of the pyrimidine−Ag_2 complex. This material is available free of charge via the Internet at http://pubs.acs.org.

References and Notes

(1) Fleischmann, M.; Hendra, P. J.; McQuillan, A. J. *Chem. Phys. Lett.* **1974**, *26*, 163.

(2) Zhao, L.; Jensen, L.; Schatz, G. C. *J. Am. Chem. Soc.* **2006**, *128*, 2911 and references therein.

(3) Creighton, J. A. The Selection Rules for Surface-Enhanced Raman Spectroscopy, in *Spectroscopy of Surfaces*; Clark, R. J. H.; Hester, R. E., Eds.; Wiley: Chichester, 1988.

(4) (a) Metiu, H. *Prog. Surf. Sci.* **1984**, *17*, 153. (b) Metiu, H. *Annu. Rev. Phys. Chem.* **1984**, *35*, 507.

(5) Lombardi, J. R.; Birke, R. L.; Lu, T.; Xu, J. *J. Chem. Phys.* **1986**, *84*, 4174 and references therein.

(6) Nie, S.; Emory, S. R. *Science* **1997**, *275*, 1102.

(7) Kneipp, K.; Wang, Y.; Kneipp, H.; Derelman, L. T.; Itzkan, I. *Phys. Rev. Lett.* **1997**, *78*, 1667.

(8) Doering, W. E., Nie, S. *J. Phys. Chem. B* **2002**, *106*, 311.

(9) Sharaabi, Y.; Shegai, T.; Haran, G. *Chem. Phys.* **2005**, *318*, 44.

(10) Kneipp, K.; Wang, Y.; Kneipp, H.; Itzkan, I.; Dasari, R. R.; Feld, M. S. *Phys. Rev. Lett.* **1996**, *76*, 2444.

(11) Haslet, T. L.; Tay, L.; Moskovits, M. *J. Chem. Phys.* **2000**, *113*, 1641.

(12) Zylka, G.; Otto, A. Search for the Dynamic Charge Transfer Excitations in Surface Enhanced Raman Scattering, in *Progress in Surface Raman Scattering*; Tian, Z. Q.; Ren, B., Eds.; Xiamen University Press: Xiamen, 2000, and references therein.

(13) See, for instance: (a) Avouris, Ph.; Dermuth, J. E. *J. Chem. Phys.* **1981**, *75*, 4783. (b) Schmeisser, D.; Demuth, J. E. *Chem. Phys. Lett.* **1982**, *87*, 32. (c) Avouris, Ph.; Demuth, J. E. *Annu. Rev. Phys. Chem.* **1984**, *35*, 49. (d) Yamada, H.; Nagaka, H.; Toba, K.; Nakao, Y. *J. Electron Spectrosc. Relat. Phenom.* **1987**, *45*, 113. (e) Yamada, H.; Nagaka, H.; Toba, K.; Nakao, Y. *Surf. Sci.* **1987**, *182*, 269. (f) Campion, A.; Ivanecky, J. E.; Child, C. M.; Foster, M. *J. Am. Chem. Soc.* **1995**, *117*, 11807.

(14) (a) Arenas, J. F.; Woolley, M. S.; Otero, J. C.; Marcos, J. I. *J. Phys. Chem.* **1996**, *100*, 3199. (b) Arenas, J. F.; López Tocón, I.; Otero, J. C.; Marcos, J. I. *J. Phys. Chem.* **1996**, *100*, 9254. (c) Arenas, J. F.; Woolley, M. S.; López Tocón, I.; Otero, J. C.; Marcos, J. I. *J. Chem. Phys.* **2000**, *112*, 7669. (d) Arenas, J. F.; Soto, J.; López Tocón, I.; Fernández, D. J.; Otero, J. C.; Marcos, J. I. *J. Chem. Phys.* **2002**, *116*, 7207. (e) Soto, J.; Fernández, D. J.; Centeno, S. P.; López Tocón, I.; Otero, J. C. *Langmuir* **2002**, *18*, 3100. (f) Arenas, J. F.; Fernández, D. J.; Soto, J.; López Tocón, I.; Otero, J. C. *J. Phys. Chem. B* **2003**, *107*, 13143. (g) Arenas, J. F.; López Tocón, I.; Castro, J. L.; Centeno, S. P.; López-Ramírez, M. R.; Otero, J. C. *J. Raman Spectrosc.* **2005**, *36*, 515. (h) Castro, J. L.; Arenas, J. F.; López-Ramírez, M. R.; Otero, J. C. *Biopolymers* **2006**, *82*, 379 and references therein.

(15) Clark, R. J. H.; Dines, T. J. *Angew. Chem., Int. Ed. Engl.* **1986**, *25*, 131.

(16) See for instance, (a) Sinclair, T. J. in *Raman spectra of the diazines at a silver electrode*, *VIIth International Conference on Raman Spectroscopy*; Heyns, A. M. Ed.; Wiley: Chichester, 1980. (b) Creighton, J. A. *Surf. Sci.* **1986**, *173*, 665. (c) Moskovits, M.; DiLella, D. P.; Maynard, K. J. *Langmuir* **1988**, *4*, 67. (d) Muniz-Miranda, M.; Neto, N.; Sbrana, G. *J. Phys. Chem.* **1988**, *92*, 954.

(17) Nenner, I.; Schulz, G. J. *J. Chem. Phys.* **1975**, *62*, 1747.

(18) Dunning, T. H., Jr.; Hay, P. J. In *Modern Theoretical Chemistry*; Schaefer, H. F., III, Ed., Plenum: New York, 1976.

(19) (a) Hay, P. J.; Wadt, W. R. *J. Chem. Phys.* **1985**, *82*, 270; (b) Hay, P. J.; Wadt, W. R. *J. Chem. Phys.* **1985**, *82*, 284; (c) Hay, P. J.; Wadt, W. R. *J. Chem. Phys.* **1985**, *82*, 299.

(20) (a) Otto, A.; Timper, J.; Billman, J.; Kovacs, G.; Pockrand, I. *Surf. Sci.* **1980**, *92*, L55. (b) Otto, A.; Pockrand, I.; Billmann, J.; Pettenkofer, C. The Adatom Model: How Important Is Atomic Scale Roughness? in *Surface-Enhanced Raman Scattering*; Chang, R. K., Furtak, T. E., Eds.; Plenum Press: New York, 1982.

(21) Foresman, J. B.; Head-Gordon, M.; Pople, J. A., Frisch, M. J. *J. Phys. Chem.* **1992**, *96*, 135.

(22) Frisch, M. J.; Trucks, G. W.; Schlegel, H. B.; Scuseria, G. E.; Robb, M. A.; Cheeseman, J. R.; Zakrzewski, V. G.; Montgomery, J. A., Jr.; Stratmann, R. E.; Burant, J. C.; Dapprich, S.; Millam, J. M.; Daniels, A. D.; Kudin, K. N.; Strain, M. C.; Farkas, O.; Tomasi, J.; Barone, V.; Cossi, M.; Cammi, R.; Mennucci, B.; Pomelli, C.; Adamo, C.; Clifford, S.; Ochterski, J.; Petersson, G. A.; Ayala, P. Y.; Cui, Q.; Morokuma, K.; Malick, D. K.; Rabuck, A. D.; Raghavachari, K.; Foresman, J. B.; Cioslowski, J.; Ortiz, J. V.; Baboul, A. G.; Stefanov, B. B.; Liu, G.; Liashenko, A.; Piskorz, P.; Komaromi, I.; Gomperts, R.; Martin, R. L.; Fox, D. J.; Keith, T.; Al-Laham, M. A.; Peng, C. Y.; Nanayakkara, A.; Gonzalez, C.; Challacombe, M.; Gill, P. M. W.; Johnson, B. G.; Chen, W.; Wong, M. W.; Andres, J. L.; Head-Gordon, M.; Replogle, E. S.; Pople, J. A. *Gaussian 98*, revision A.7; Gaussian, Inc.: Pittsburgh, PA, 1998.

(23) Peticolas, W. L.; Strommen, D. P.; Lakshminarayanan, V. *J. Chem. Phys.* **1980**, *73*, 4185 and references therein.

(24) Pulay, P.; Fogarasi, G.; Boggs, J. E. *J. Chem. Phys.* **1981**, *74*, 3999.

(25) (a) Sbrana, G.; Adembri, G.; Califano, S. *Spectrochim. Acta* **1966**, *22*, 1831. (b) Milani-Nejad, F.; Stidham, H. D. *Spectrochim. Acta* **1975**, *31A*, 1433. (c) Bokobza-Sebagh, L.; Zarembowitch, J. *Spectrochim. Acta* **1976**, *32A*, 797. (d) Pongor, G.; Fogarasi, G.; Magdó, I.; Boggs, J. E.; Keresztury, G.; Ignatyev, I. S. *Spectrochim. Acta* **1992**, *48A*, 111.

(26) Vivoni, A.; Birke, R. L.; Foucault, R.; Lombardi, J. R. *J. Phys. Chem. B* **2003**, *107*, 5547.

(27) For instance, CIS/LanL2DZ energies of S_1 states of pyrazine and pyridine[14d] are 4.70 and 5.21 eV, while experimental values amount to 3.83 (Zhu, L.; Johnson, P. *J. Chem. Phys.* **1993**, *99*, 2322) and 4.31 (Mochizuki, Y.; Kaya, K.; Ito, M. *J. Che. Phys.* **1976**, *65*, 4163) eV, respectively).